RSC Advances

PAPER

View Article Online
View Journal | View Issue

Cite this: *RSC Adv.*, 2026, **16**, 4363

A new method for the synthesis of 6,7-dihydro-5*H*-pyrrolo[2,1-*a*][2]benzazepines and 5,6,7,9,10,11-hexahydro-12*H*-indolo[2,1-*a*][2]benzazepines and evaluation of their bioactivity

Alisa A. Nevskaya,*[ab] Tuyet Anh Dang Thi,*[c] Tatiana N. Borisova,[a] Alexander A. Titov,[a] Lada V. Anikina,[e] Elena Yu. Nevskaya,[b] Alexey V. Varlamov,[a] Leonid G. Voskressensky[a] and Le Tuan Anh[d]

Received 21st November 2025
Accepted 9th January 2026

DOI: 10.1039/d5ra09014h

rsc.li/rsc-advances

This article describes a new method for the synthesis of pyrrolo[2,1-*a*][2]benzazepine and indolo[2,1-*a*][2]benzazepine derivatives with different pyrrole fragment structures containing functional groups. The method is based on domino reactions involving the imino-ketone fragment of 1-aroyl-4,5-dihydro-3*H*-[2]benzazepines and electron-deficient alkenes and alkynes. The anticancer and anti-inflammatory activities of synthesized compounds were evaluated. These compounds displayed significant toxicity to four cancer cell lines (including RD, HCT116, HeLa and A549 ones). Amongst these compounds, **3b–e** had the best inhibitory activity against the tested cancer cell lines with IC_{50} values ranging from 4.52 to 19.97 μM, Notably, compound **3b** demonstrated the most potent inhibitory effect on nitric oxide (NO) production, with an IC value of only slightly higher than those of the reference compound L-NMMA. Furthermore, molecular docking studies revealed the important interaction of four compounds **3b–e** with residues in the etoposide-binding site of topoisomerase as well.

Introduction

The pyrrolobenzazepine moiety is part of a number of alkaloids that exhibit various biological activities. There are a limited number of studies in the literature devoted to the synthesis of pyrrolobenzazepines. Of the four types of pyrrolobenzazepines with a fusion of the pyrrole and benzazepine moieties—pyrrolo[1,2-*a*][1]benzazepines, pyrrolo[1,2-*b*][2]benzazepines, pyrrolo[2,1-*b*][3]benzazepines, and pyrrolo[2,1-*a*][2]benzazepines—the latter have been partially studied.

The pyrrolo[2,1-*a*][2]benzazepine moiety is the structural component of homoerythrine alkaloids (Fig. 1). These alkaloids are known for their anxiolytic and CNS depressant activity, and there is also evidence of other pharmacological properties such as analgesic, anti-inflammatory, and antimicrobial activity.[1,2]

This series of compounds attracts researchers due to their wide range of biological properties. Compounds are known to exhibit activity against lymphoid leukemia P-388 *in vivo*,[3] and also as hepatitis C inhibitors.[4] The search for new methods for the synthesis of 6,7-dihydro-5*H*-pyrrolo[2,1-*a*][2]benzazepines, which are promising and interesting compounds in terms of biological activity, is a pressing issue in heterocyclic chemistry.

Below are three strategies for the synthesis of pyrrolo[2,1-*a*][2]benzazepines proposed by different groups of scientists to date (Scheme 1), which describe the formation of either an azepine or a pyrrole ring during the construction of the target

[a]*Organic Chemistry Department, RUDN University, 6 Miklukho-Maklaya St., Moscow 117198, Russia. E-mail: nevskaya_aa@pfur.ru*
[b]*General and Inorganic Chemistry Department, RUDN University, 6 Miklukho-Maklaya St., Moscow 117198, Russia*
[c]*Institute of Chemistry, Vietnam Academy of Science and Technology (VAST), 18 Hoang Quoc Viet Street, Nghia Do Ward, Hanoi, Vietnam. E-mail: dangtuyetanh1201@gmail.com*
[d]*Faculty of Chemistry University of Science, Vietnam National University Hanoi, 19 Le Thanh Tong, Hanoi, Vietnam*
[e]*Institute of Physiologically Active Compounds at Federal Research Center of Problems of Chemical Physics and Medicinal Chemistry, Russian Academy of Sciences (IPAC RAS), Severniy Proezd 1, Chernogolovka, 142432, Moscow Region, Russia*

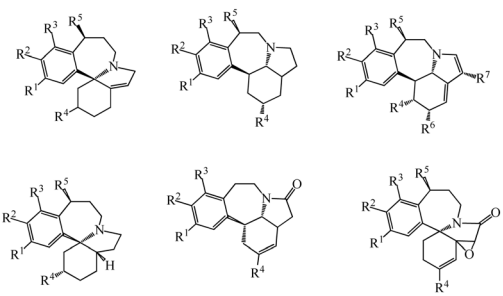

Fig. 1 Homoerythrine alkaloids.

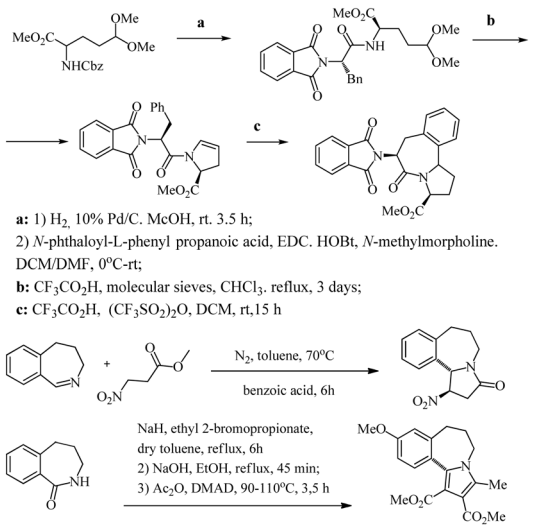

Scheme 1 The synthesis of pyrrolobenzazepines.

pyrrolobenzazepine framework: intramolecular cyclization catalyzed by $TiCl_2$;[5] intramolecular Schmidt reaction;[6] cyclization of *N*-substituted pyrrole derivatives according to Friedel–Crafts.[7] More details on the synthetic methods and biological properties of pyrrolo[2,1-*a*][2]benzazepines can be found in a 2025 review.[8]

Results and discussion

For several years, our group has been studying domino reactions of fused heterocyclic compounds with six- or seven-membered fragments containing an imino-ketone group, involving conjugated electron-deficient alkenes and alkynes. Aroyl derivatives of isoquinolines,[9–11] benzo[*h*]isoquinolines,[12] thieno[3,2-*c*]pyridines,[13] β-carbolines,[14] and pyrrolo[1,2-*a*][1,4]benzodiazepines[15] have been studied in these transformations.

We propose that the first step in the domino reaction of heterocyclic compounds containing an imino-ketone moiety with electron-deficient alkenes involves the formation of a Michael type zwitterion **A** (Scheme 2). Then the carbanion center attacks the carbon atom of the carbonyl group, leading to the closure of the five-membered ring (intermediate **B**). In the final stage of the transformations with alkenes, dehydration and aromatization lead to the formation of a pyrrole ring (Scheme 2). In reactions with alkynes, the process culminates in

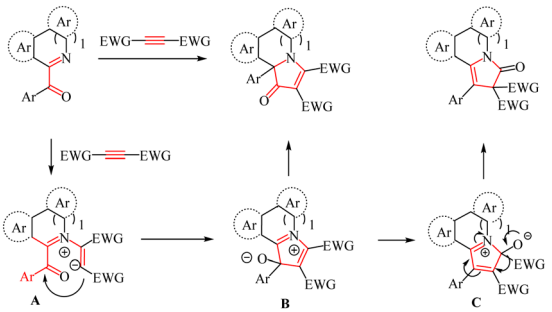

Scheme 3 The proposed reaction mechanism with alkynes.

two types of rearrangements (Scheme 3), yielding five-membered rings with different structures and vicinal or geminal functional groups.[10,11]

A two-component reaction of 1-aroyl-4,5-dihydro-3*H*-[2]benzazepines with a series of electron-deficient alkenes and alkynes was used to synthesize 6,7-dihydro-5*H*-pyrrolo[2,1-*a*][2]benzazepines and 5,6,7,9,10,11-hexahydro-12*H*-indolo[2,1-*a*][2]benzazepines. This method has not been used previously and may serve as a new approach for the preparation of 6,7-dihydro-5*H*-pyrrolo[2,1-*a*][2]benzazepines and 5,6,7,9,10,11-hexahydro-12*H*-indolo[2,1-*a*][2]benzazepine derivatives.

1-Aroyl-4,5-dihydro-3*H*-[2]benzazepines **2a,b**, having an imino-ketone fragment, were obtained according to a known method[16] by cyclization of dimethoxyphenylpropylamides of aroylformic acids in the presence of phosphorus oxychloride (Scheme 4). It was found that this method is optimal for the synthesis of benzazepine derivatives containing methoxy groups. The presence of electron-donating methoxy groups facilitates electrophilic substitution reactions in the synthesis of benzazepines from the corresponding amides. Furthermore, the presence of methoxy groups generally provides a higher level of bioactivity, increasing affinity of the synthesized molecules for biological targets.

Aroyl-substituted benzazepines **2a,b** were reacted with electron-deficient alkenes: acrolein, methyl vinyl ketone, cinnamaldehyde, cyclohexenone in trifluoroethanol and with *p*-nitrophenyl acrylate in toluene at 40 °C. As a result of the transformation, 6,7-dihydro-5*H*-pyrrolo[2,1-*a*][2]benzazepines **3a–g** and 5,6,7,9,10,11-hexahydro-12*H*-indolo[2,1-*a*][2]benzazepines **3h,i** were obtained in yields of 42–86% (Scheme 5).

Reaction conditions were optimized for the transformation of benzazepine **2a** and methyl vinyl ketone to produce pyrrolo

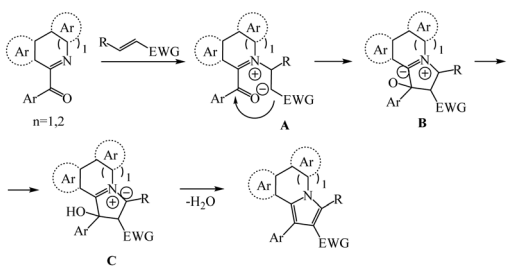

Scheme 2 The proposed reaction mechanism with alkenes.

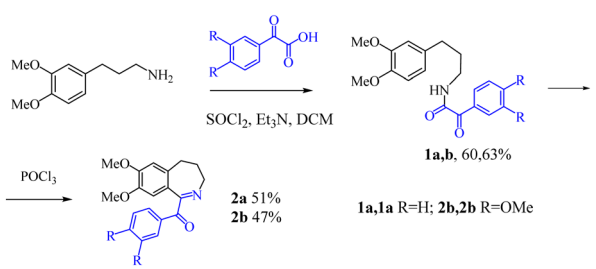

Scheme 4 Synthesis of aroyl-substituted benzazepines **2a,b**.

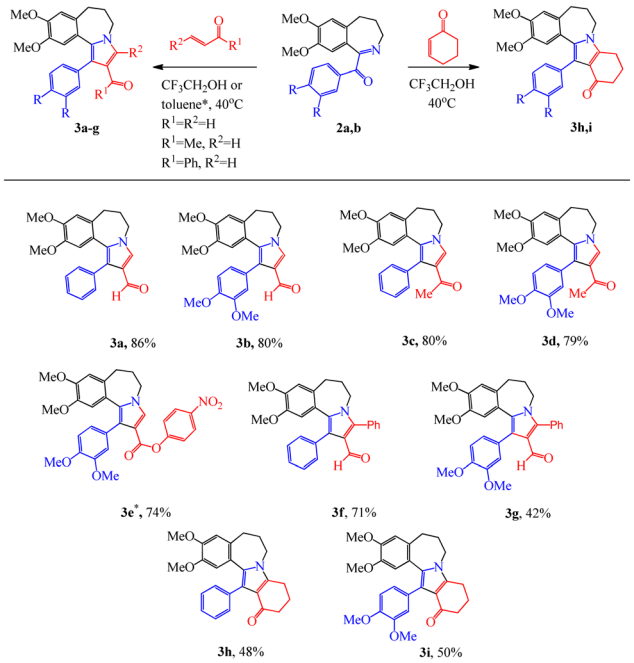

Scheme 5 Synthesis of 6,7-dihydro-5*H*-pyrrolo[2,1-*a*][2]benzazepines **3a–g** and 5,6,7,9,10,11-hexahydro-12*H*-indolo[2,1-*a*][2]benzazepines **3h,i**.

Table 1 Optimization of the reaction conditions of benzazepine **2a** and methyl vinyl ketone

Conditions	Result
r.t., CH_3CN	No reaction
Reflux, CH_3CN	No reaction
100 °C, CH_3CN, MW	Decomposition
r.t., CH_3CH_2OH	**3c** (24%)
40 °C, CH_3CH_2OH	**3c** (25%)
r.t., CF_3CH_2OH	**3c** (60%)
40 °C, CF_3CH_2OH	**3c** (80%)

[2,1-*a*][2]benzazepine **3c** (Table 1). It studies revealed that the reaction did not proceed in acetonitrile. Replacement of the solvent with ethanol or 2,2,2-trifluoroethanol resulted in the interaction, but in trifluoroethanol the reaction proceeds with an increased yield of **3c**.

We propose that the reaction of 1-aroylbenzazepines **2a,b** with electron-deficient alkenes begins with the formation of zwitterion **A**, which is converted into zwitterion **B** *via* a Michael addition. This latter intermediate, through ylide **C**, yields 6,7-dihydro-5*H*-pyrrolo[2,1-*a*][2]benzazepines **3a–g** and 5,6,7,9,10,11-hexahydro-12*H*-indolo[2,1-*a*][2]benzazepines **3h,i** (Scheme 6).

For compound **3a**, Fig. 2 presents X-ray diffraction data, which provide additional confirmation for the structure of the obtained 6,7-dihydro-5*H*-pyrrolo[2,1-*a*][2]benzazepines.

We also conducted reactions of benzazepine **2a** with a number of alkenes, such as crotonic aldehyde, acrylonitrile and ethyl acrylate under various conditions. However, we were

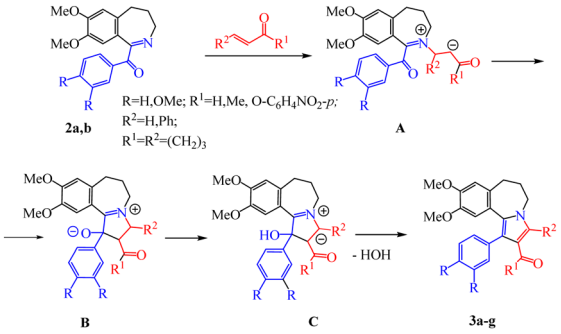

Scheme 6 Synthesis of 6,7-dihydro-5*H*-pyrrolo[2,1-*a*][2]benzazepines **3a–g**.

Fig. 2 Molecular structure of compound **3a**.

unable to isolate the expected products. A table of optimization conditions is provided in the SI (Table S1).

1-Aroyl-4,5-dihydro-3*H*-[2]benzazepines **2a,b** react with electron-deficient alkynes—dimethyl acetylenedicarboxylate and acetylacetylene (Scheme 7)—under microwave irradiation in acetonitrile at 150 °C. It has been established that the domino reactions of benzazepines **2a,b** with acetylacetylene and dimethyl acetylenedicarboxylate are accompanied by a skeletal rearrangement involving the transfer of an aryl group to the 11b position and the formation of a pyrrolinone cycle. As a result, 6,7-dihydro-5*H*-pyrrolo[2,1-*a*][2]benzazepines **4a–c** were obtained (Scheme 7).

Benzazepines **4a–c** obtained by reaction with alkynes are formed as a racemate. Reaction conditions were optimized for the transformation of benzazepine **2a** and acetylenedicarboxylate to produce pyrrolo[2,1-*a*][2]benzazepine **4c** (Table 2).

The proposed mechanism of the process is shown in Scheme 8. We suggest that the reaction proceeds *via* the formation of zwitterion **A**. After the pyrrole ring closure and the formation of intermediate **B**, two pathways are possible. In the first case,

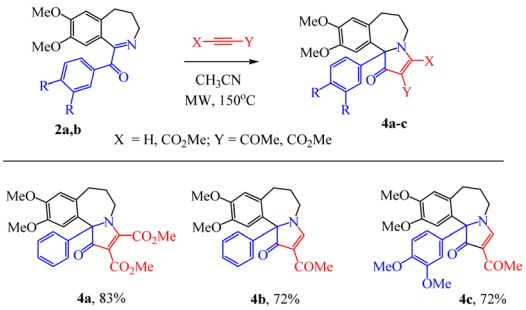

Scheme 7 Synthesis of 6,7-dihydro-5*H*-pyrrolo[2,1-*a*][2]benzazepines **4a–c**.

Table 2 Optimization of the reaction conditions of benzazepine **2a** and acetylenedicarboxylate

Conditions	Result
40 °C, CF_3CH_2OH	Multicomponent inseparable mixture
Reflux, CH_3CN	No reaction
Reflux, CH_3CN	**3c** (60%)
150 °C, CH_3CN, MW	**3c** (72%)

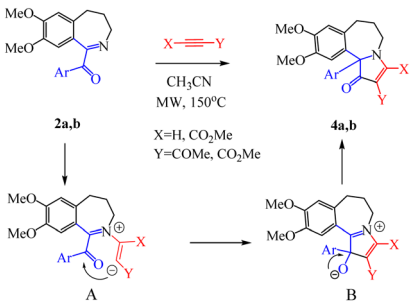

Scheme 8 Plausible mechanism for the synthesis of 6,7-dihydro-5*H*-pyrrolo[2,1-*a*][2]benzazepines **4a,b**.

transfer of the aryl group to the 11b position occurs, leading to the formation of a five-membered ring with a cross-conjugated system – 6,7-dihydro-5*H*-pyrrolo[2,1-*a*][2]benzazepines **4a–c** with vicinally positioned functional groups. Similar transformations with internal alkynes were observed for all series of compounds studied by us.[9,17]

As a result, a convenient and accessible synthesis of 6,7-dihydro-5*H*-pyrrolo[2,1-*a*][2]benzazepine and 5,6,7,9,10,11-hexahydro-12*H*-indolo[2,1-*a*][2]benzazepine derivatives has been developed. This synthesis is based on domino reactions of 1-aroyl-4,5-dihydro-3*H*-[2]benzazepines containing an iminoketone fragment with electron-deficient alkenes and alkynes. While the reaction with alkenes leads to the annulation of an aromatic pyrrole cycle, the transformations involving alkynes are characterized by rearrangement and the appearance of a carbonyl group in a non-aromatic five-membered ring.

The biological activity of the synthesized compounds was assessed, including screening for cytotoxic activity, inhibition of NO production, and molecular docking with topoisomerase IIb.

Cytotoxicity of synthesized compounds

The obtained compounds 6,7-dihydro-5*H*-pyrrolo[2,1-*a*][2]benzazepines **3a–g**, **4a** and 5,6,7,9,10,11-hexahydro-12*H*-indolo[2,1-*a*][2]benzazepines **3h,i** underwent primary bioscreening to assess cytotoxic activity using the MTT assay (tetrazolium dye colorimetric assay). The testing was conducted at the Federal State Budgetary Institution "Institute of Physiologically Active Compounds of the Russian Academy of Sciences (IPAC RAS)" by Senior Researcher L. V. Anikina. The primary evaluation of the compounds' cytotoxic activity was performed on the following human cell cultures: A549 (lung carcinoma), HCT116 (colorectal carcinoma), RD (rhabdomyosarcoma), and HeLa (cervical adenocarcinoma). Daunorubicin was used as positive control and the results are summarized in Table 3.

These results indicate that most of the derivatives possess at least moderate cytotoxic activity, and some benzazepines even display a promising activity profile. In particular, four 6,7-dihydro-5*H*-pyrrolo[2,1-*a*][2]benzazepines (**3b–e**) displayed good inhibitory effects against all four tested cell lines with IC_{50}-values ranging from 4.52 to 19.97 μM, and a higher susceptibility were found in HCT116 and HeLa proliferation. Three benzazepines compounds (**3f**, **3i**, and **4a**) exhibit considerable cytotoxicity against HeLa and A549 cancer cell lines with IC_{50} values < 50 μM, pointing to the potential interest in this new class of benzazepines molecules. The 6,7-dihydro-5*H*-pyrrolo[2,1-*a*][2]benzazepines **3b** can be identified as the most promising compound with IC_{50}-values below 5 μM against both HTC116 and A549 cell lines (4.52 and 4.55 μM, respectively), only slightly higher than those of the reference compound daunorubicin, thus representing a suitable template for further elaboration and optimization toward potent cytotoxic agents (Table 3).

In vitro anti-inflammatory effects based on the inhibition of NO

The anti-inflammatory activity of products **3a–b**, **3d–g**, **3i**, **2a–b**, **1a** was evaluated by NO assay, and their effect on the viability of

Table 3 Cytotoxicity of the products against RD, HTC116, HeLa and A549 cell lines

			IC_{50} (μM)			
Entry	Compound	R, R^1, R^2, X, Y	RD	HCT116	HeLa	A549
1	**3a**	R, R^1, R^2 = H	669.79 ± 28.18	207.55 ± 7.69	—	—
2	**3b**	R = OMe, R^1 = H, R^2 = H	**10.56 ± 0.86**	**4.52 ± 0.63**	**6.89 ± 0.51**	**4.55 ± 0.13**
3	**3c**	R = H, R^1 = Me, R^2 = H	**11.67 ± 0.40**	**5.83 ± 0.37**	**5.61 ± 0.36**	**19.32 ± 1.93**
4	**3d**	R = OMe, R^1 = Me, R^2 = H	**10.38 ± 0.25**	**6.03 ± 0.24**	**5.98 ± 0.30**	**8.83 ± 0.64**
5	**3e**	R = OMe, R^1 = O–$C_6H_5NO_2$-*p*, R^2 = H	**19.97 ± 1.56**	**6.99 ± 0.43**	**7.35 ± 0.19**	**7.56 ± 0.39**
6	**3f**	R = H, R^1 = H, R^2 = Ph	148.03 ± 9.49	119.88 ± 6.39	101.21 ± 4.46	104.29 ± 6.10
7	**3g**	R = OMe, R^1 = H, R^2 = Ph	448.08 ± 19.25	394.57 ± 11.14	401.37 ± 50.08	126.10 ± 12.15
8	**3h**	R = H, R^1 = R^2 = $(CH_2)_3$	403.31 ± 14.55	553.23 ± 22.07	375.89 ± 17.73	148.65 ± 7.48
9	**3i**	R = OMe, R^1 = R^2 = $(CH_2)_3$	146.32 ± 8.98	100.50 ± 5.93	90.49 ± 4.28	45.66 ± 3.49
10	**4a**	R = H, X = CO_2Me, Y = CO_2Me	100.15 ± 9.81	51.19 ± 2.92	48.26 ± 4.21	76.74 ± 2.30
11	Daunorubicin		0.33 ± 0.01	0.29 ± 0.01	0.28 ± 0.02	0.53 ± 0.05

Table 4 Effects of the synthesized compounds on the cell viability of RAW 264.7 cells

		Cell viability (%)			
Product	R, R^1, R^2	256 μg ml^{-1}	64 μg ml^{-1}	16 μg ml^{-1}	4 μg ml^{-1}
3a	R, R^1, R^2 = H	27	30	46	63
3b	R = OMe, R^1 = H, R^2 = H	5	67	80	84
3d	R = OMe, R^1 = Me, R^2 = H	3	67	75	78
3e	R = OMe, R^2 = H, R^1 = $OC_6H_5NO_2$-*p*	7	57	61	87
3g	R = OMe, R^1 = H, R^2 = Ph	86	90	93	95
3i	R = OMe, R^1 = R^2 = $(CH_2)_3$	84	90	95	96
2a	R = H	1	86	95	100
2b	R = OMe	82	92	99	100
1a	R = H	15	96	99	100
L-NMMA		82	75	72	50

RAW 264.7 cell was assessed by MTT (3-(4,5-dimethylthiazol-2-yl)-2,5-diphenyl-tetrazolium bromide) assay. The cells were pre-treated with compounds **3a–b**, **3d–g**, **3i**, **2a–b**, **1a** at the concentrations of 256, 64, 16, and 2 μg ml^{-1}. The results revealed that at concentration of 256 μg ml^{-1}, the viability of RAW 264.7 cells was found to be less than 7%, thus the inhibition effect of products at this concentration was not measured (Table 4). Cytotoxic effect decreased with lower concentrations (Fig. 3). At a concentration of 4 μg ml^{-1}, the compounds (**3b**, **3g**, **3i**, **2a**, **1a**) could inhibit NO production with values of 40, 29, 48, 35, and 23%, respectively. At a concentration of 16 μg ml^{-1}, compounds (**3b**, **3i**) and (**2a**) had a good ability to block NO production by 63, 50%, and 75% respectively (Fig. 3). These 6,7-dihydro-5*H*-pyrrolo[2,1-*a*][2]benzazepines (**3g**), aroyl-substituted benzazepines (**2b**) and 2-oxoacetamides (**1a**), at 16 μg ml^{-1}, only partially inhibited the generation of NO by 42, 9,

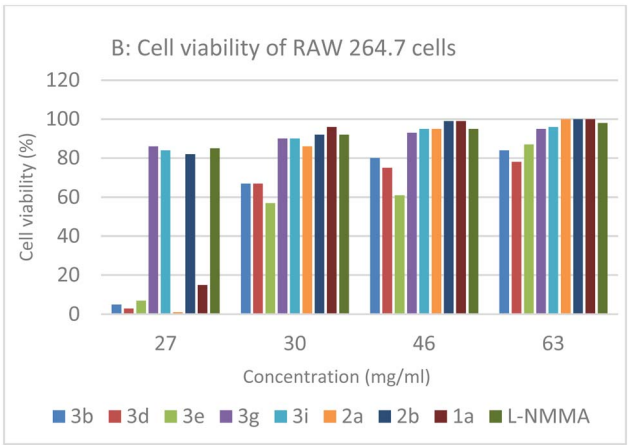

Fig. 3 Inhibitory effect of **3a–b**, **3d–g**, **3i**, **2a–b**, **1a** on cell viability of RAW 264.7 cells.

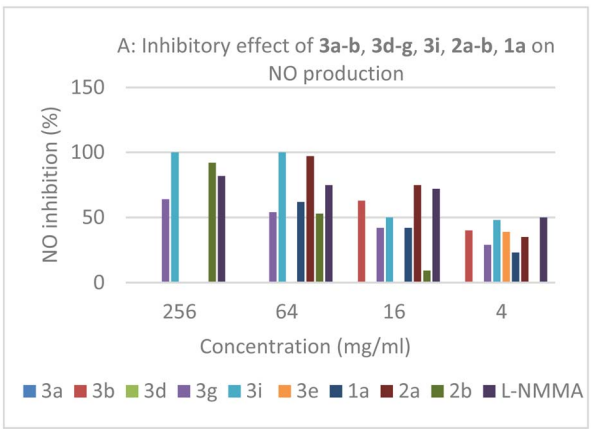

Fig. 4 Effect of products **3a–b**, **3d–g**, **3i**, **2a–b**, **1a** on NO in LPS-mediated macrophage RAW 264.7 cells.

Table 5 Half-maximal inhibitory concentration (IC_{50}, μM, μg ml^{-1}) of products **3a–b**, **3d–g**, **3i**, **2a–b**, **1a** against NO assay

Compound	R, R^1, R^2	IC_{50} (μg ml^{-1})	IC_{50} (μM)
3a	R, R^1, R^2 = H	ND	ND
3b	R = OMe, R^1 = H, R^2 = H	**7.79 ± 0.5**	**19.1 ± 1.2**
3d	R = OMe, R^1 = Me, R^2 = H	ND	ND
3e	R = OMe, R^1 = O–$C_6H_5NO_2$-*p*, R^2 = H	>256	ND
3g	R = OMe, R^1 = H, R^2 = Ph	48.0 ± 3.22	99.2 ± 6.6
3i	R = OMe, R^1 = R^2 = $(CH_2)_3$	16.0 ± 1.5	35.7 ± 3.4
2a	R = H	**8.5 ± 0.5**	**27.4 ± 1.6**
2b	R = OMe	60.7 ± 4.2	164.5 ± 11.4
1a	R = H	35.2 ± 2.2	107.5 ± 6.9
L-NMMA		4.0 ± 0.5	16.1 ± 2.0

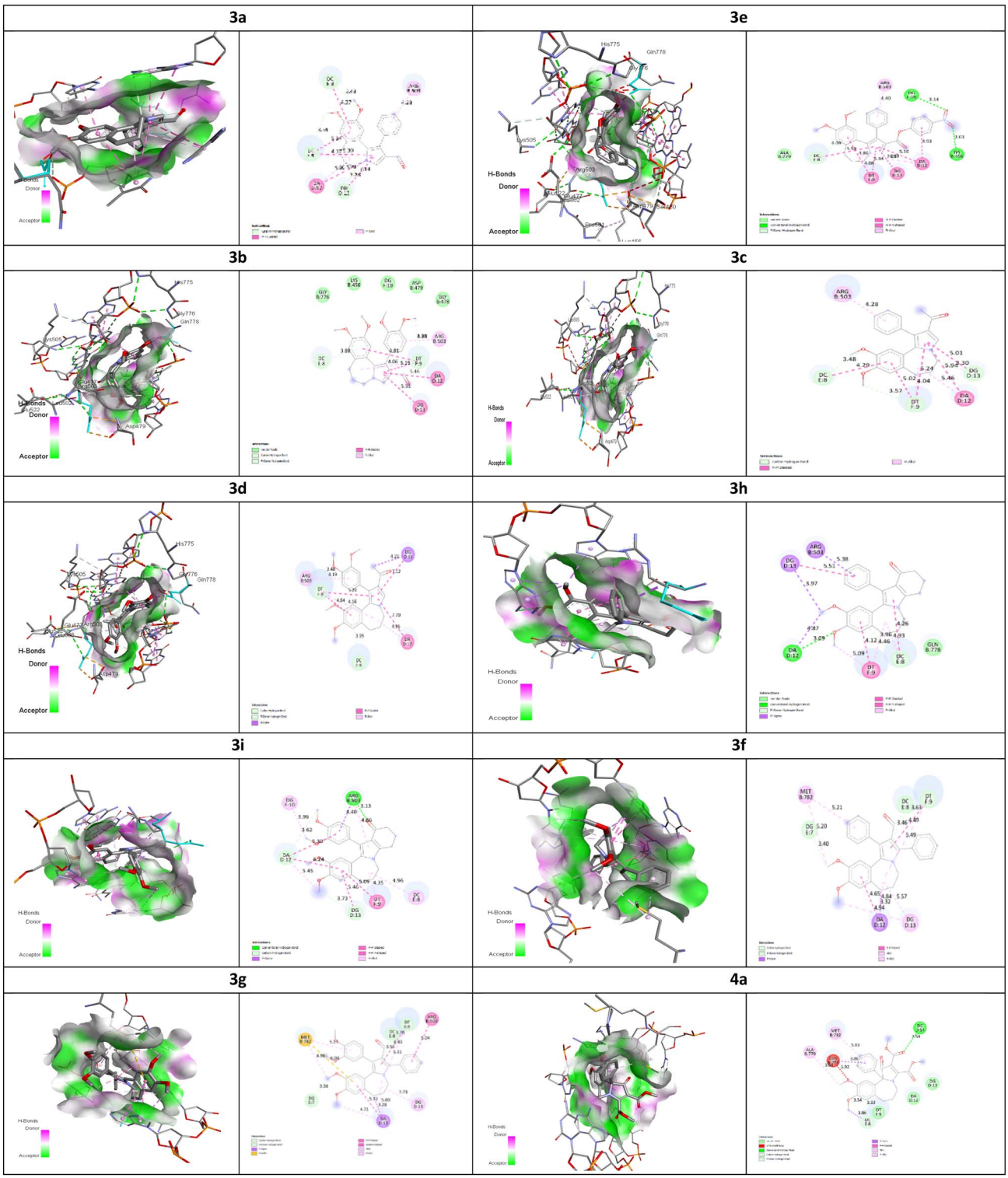

Fig. 5 The 3D and 2D interactions of ten potential inhibitors, coligand (EPV) with the receptor 3QX3.

and 42% respectively. As depicted in Table 5 and Fig. 4, most of these derivatives possessed moderate NO inhibitory activity against lipopolysaccharide (LPS)-induced nitric oxide release with the IC_{50} values in the range of 19.1–164.5 μM. Among tested compounds, product **3b** was found to be the best at blocking NO with an IC_{50} value of 19.1 ± 1.2 μM, only slightly higher than those of the reference compound L-NMMA (Fig. 3 and 4).

Molecular modeling

On the grounds of cytotoxic evaluation, it is of interest studying the interactions between products against potential anticancer

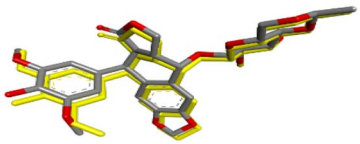

Fig. 6 Redocked poses and original poses of EPV (yellow).

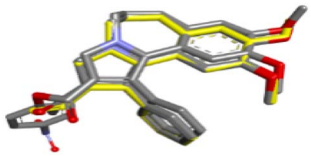

Fig. 7 Docking poses of **3a–e** in the EPV binding site.

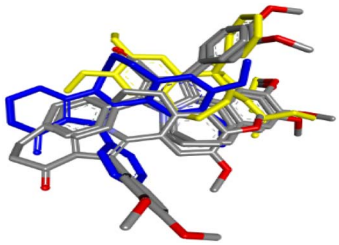

Fig. 8 Docking poses of **4a** (yellow), **3h** (blue) and **3f–g**, **3i** in the EPV binding site.

dual targets, such as topoisomerase. In this study, as a standard protocol, etoposide (EPV) were redocked to validate the docking method before applying it to the investigated synthesized compounds (Fig. 6). The binding energy of synthesized compounds ranged from −7.4 to −10.5 (kcal mol^{-1}). They could be divided into two groups. Group I includes compounds **3a–3d** and **3e**. They aligned in the same conformation in the binding pocket of protein (Fig. 7). They displayed some common features, such as inhibition of topoisomerase by intercalating the DNA through the main interactions of carbon-hydrogen bonds with DC8, DT9, DG13; pi–pi stacked bonds with DC8, DT9, DG13, DA12; and pi–alkyl bonds with DT9, DA12 Arg503 (Fig. 5). The benzene ring attached to the pyrrole ring in these compounds always interacts with the receptor by pi–alkyl bond with Arg503, as observed in the case of EPV, but with differing distances, in which the shortest distance belongs to compound **3d** (4.19 Å) followed by compound **3b**, compounds **3c** and **3a** (4.28 Å), and compound **3e** (4.40 Å). The lowest negative value of docking score belongs to compound **3e**, which reflects notable binding of **3e** with the active site of the protein.

Interestingly, compounds **3b–3d** and **3e** have better binding affinity than **3a** due to the presence of different substitutions. For example, the introduction of 4-nitrophenol resulted in the formation of two conventional hydrogen bonds with DG10 and Lys456 (compound **3e**). These interactions may contribute to the increased stability and enhanced binding affinity of this compound. Group II consists of compounds **3f–3i** and **4a**. They almost have the same conformation in the binding pocket, with slightly different of compound **4a** (yellow) and **3h** (blue) (Fig. 8). Compound **4a** has the highest docking score (−7.4 kcal mol^{-1}) with the fewest interactions with amino acid residues (6 interactions) (Fig. 5). The number of interactions of compounds **3f–3i** ranged from 10 to 13 (Table 6). Furthermore, molecular docking approaches have inherent limitations, such as solvent effects, flexibility of protein, and inaccurate scoring functions, which might lead to discrepancies between docking results and experimental outcomes.

Despite these obstacles, molecular docking studies could provide valuable insights into the binding modes of designed ligands. Among the newly synthesized derivatives, the compounds **3b–3e** were observed as the optimal candidates for anticancer due to their lower binding affinity (binding affinity ranged from −9.8 to −10.5 kcal mol^{-1}). A comparison of cytotoxicity evaluation results (Table 3) and docking outcomes (Table 6) suggests a good correlation between the biological activities and binding affinity of synthetic compounds. Some of our synthesized derivatives (**3b–3e**) may serve as promising scaffolds for future optimization with higher potency in tumor treatment.

Experimental

Chemistry

Materials and general procedures. All reagents and solvents were purchased from Merck, J.T. Baker, or Sigma-Aldrich

Table 6 Binding energy and bond interactions

		Interactions with amino acid residues		
Entry	Binding energy (kcal mol^{-1})	Main part	Substitution	Total interactions
3a	−8.1	DC8, DT9, DA12, DG13, ArG503		11
3b	−9.8	DC8, DT9, DA12, DG13, ArG503	DT9	8
3c	−9.9	DC8, DT9, DA12, DG13, ArG503		11
3d	−9.8	DC8, DT9, DA12, DG13, ArG503	DG13, DT9	10
3e	−10.5	DC8, DT9, DG10, DA12, DG13, ArG503, Lys456	Lys456, DG10, DA12	11
3f	−8.8	DG7, DC8, DT9, DA12, DG13, Met782	DT9	12
3g	−8.4	DG7, DC8, DT9, DA12, DG13, Arg503	DT9, Arg503	13
3h	−10.3	DC8, DT9, DA12, DG13, ArG503		10
3i	−10.2	DC8, DT9, DG10, DA12, DG13, Arg503	DG10, DA12, Arg503	13
4a	−7.4	DC8, Ala779, Glc778, Met782	DC14	6
EPV	DC8, DG10, DA12, DG13, Asp479, Gly478, Arg503, Pro819, Met782			14

Chemical Co., and were used without further purification. ^{1}H and ^{13}C NMR spectra were recorded in chloroform-d ($CDCl_3$) or dimethylsulfoxide-d_6 (DMSO-d_6) solution at 25 °C, with a 600 MHz (^{1}H) or 150 MHz (^{13}C) NMR spectrometer; peak positions are given in parts per million (δ) referenced to the appropriate solvent residual peak. Mass spectra (LC-MS) of compounds were acquired on an Agilent 1100/Agilent Technologies LC/MSD VL LC-MS system (electrospray ionization). Melting points were measured with a melting point apparatus Stuart SMP 30 in the open capillary tubes. Microwave syntheses were performed in an Anton Paar monowave 400 microwave reactor. Temperature monitoring during microwave syntheses was achieved *via* the use of an external surface temperature sensor. Column chromatography was carried out with silica gel grade 60 (0.040–0.063 mm) 230–400 mesh. Elemental analyses were carried out on Euro Vector EA-3000 Elemental Analyzer for C, H, and N; experimental data agreed to within 0.04% of the theoretical values.

Synthesis of (7,8-dimethoxy-4,5-dihydro-3*H*-2-benzazepin-1-yl)(phenyl)methanones 2a,b (general procedure). To *N*-(3-(3,4-dimethoxyphenyl)propyl)-2-oxo-2-phenylacetamides **1a,b** (0.61 mmol), $POCl_3$ (15.2 mmol) was added at 0 °C under an argon atmosphere. The reaction mixture was heated to 50 °C and stirred for 8 hours under argon. The reaction progress was monitored by TLC (Sorbfil, ethyl acetate/hexane, 2.5 : 4). The reaction mixture was poured onto ice (10 g) and neutralized with a 25% ammonia solution to a basic pH of 10. The mixture was extracted with ethyl acetate (3 × 15 ml), and the organic extract was dried over $MgSO_4$. The solvent was removed under reduced pressure to afford benzazepines **2a,b** as a yellow oil.

(7,8-Dimethoxy-4,5-dihydro-3*H*-2-benzazepin-1-yl)(phenyl) methanone (2a). Yield: 96 mg (51%), yellow oil. ^{1}H NMR (600 MHz, $CDCl_3$), δ = 2.43–2.46 (m, 2H, 4-CH_2), 2.65 (t, 2H, J = 7.3 Hz, 5-CH_2), 3.57 (t, 2H, J = 6.8 Hz, 3-CH_2), 3.82 (s, 3H, OCH_3), 3.92 (s, 3H, OCH_3), 6.78 (s, 1H, H-6), 7.00 (s, 1H, H-9), 7.45–7.48 (m, 2H, H-Ar), 7.58–7.59 (m, 1H, H-Ar), 8.04–8.05 (m, 2H, H-Ar). ^{13}C NMR (150 MHz, $CDCl_3$), δ = 30.7, 35.0, 50.6, 56.0, 56.2, 111.3, 112.0, 127.5, 128.6, 130.6, 131.2, 132.1, 133.6, 134.6, 135.8, 147.4, 150.5, 169.5, 194.0. MS (LCMS), m/z: 310 $[M + H]^+$. Found, $C_{19}H_{19}NO_3$, exact mass: 309 (%): C, 73.65; H, 6.04; N, 4.43. Anal. calcd (%): C, 73.77; H, 6.19; N, 4.53.

Synthesis of 9,10-dimethoxy-1-phenyl-6,7-dihydro-5*H*-pyrrolo[2,1-*a*][2]benzazepine-2-carbaldehydes 3a–g and 2,3-dimethoxy-13-phenyl-5,6,7,9,10,11-hexahydro-12*H*-indolo[2,1-*a*][2]benzazepin-12-ones 3h,i (general procedure). To a solution of (4,5-dihydro-3*H*-benzo[*c*]azepin-1-yl)(phenyl)methanones **2a,b** (0.16 mmol) in 2 ml of trifluoroethanol was added 0.23 mmol of an alkene: acrolein (for **3a,b**), methyl vinyl ketone (for **3c,d**), cinnamaldehyde (for **3f,g**) or cyclohexenone (for **3h,i**). The reaction was carried out at 40 °C, the reaction progress was monitored by TLC (Sorbfil, ethyl acetate–hexane, 2 : 1). After removing the solvent, the reaction mixture was purified by column chromatography (aluminum oxide, ethyl acetate–petroleum ether, 1 : 10).

9,10-Dimethoxy-1-phenyl-6,7-dihydro-5*H*-pyrrolo[2,1-*a*][2] benzazepine-2-carbaldehyde (3a). Yield: 48 mg (86%), white powder, mp 180–182 °C. ^{1}H NMR (600 MHz, $CDCl_3$), δ = 2.26–2.28 (m, 2H, 6-CH_2), 2.73 (t, 2H, J = 7.1 Hz, 7-CH_2), 3.36 (s, 3H, OCH_3), 3.89 (s, 3H, OCH_3), 3.91 (t, 2H, J = 6.8 Hz, 5-CH_2), 6.31 (s, 1H, H-11), 6.76 (s, 1H, H-8), 7.23–7.30 (m, 5H, H-Ar), 7.49 (s, 1H, H-3), 9.78 (s, 1H, CHO). ^{13}C NMR (150 MHz, $CDCl_3$), δ = 30.3, 31.2, 46.5, 55.6, 56.0, 112.3, 113.2, 122.9, 123.3, 126.5, 126.8, 128.3 (2C), 130.8 (2C), 130.9, 132.7, 133.6, 147.2, 148.5, 185.0, 186.7. MS (LCMS), m/z: 348 $[M + H]^+$. Found, $C_{22}H_{21}NO_3$, exact mass: 347 (%): C, 75.91; H, 6.12; N, 3.94. Anal. calcd (%): C, 76.06; H, 6.09; N, 4.03.

9,10-Dimethoxy-1-oxo-11b-phenyl-5,6,7,11b-tetrahydro-1*H*-pyrrolo[2,1-*a*][2]benzazepine-2-carboxylates (4a–c). To a solution of 77 mg (0.25 mmol) of compound **2a,b** in 5 ml of acetonitrile, 0.42 mmol of acetylenedicarboxylate (for **4a**) or but-3-yn-2-one (for **4b,c**) was added. The reaction was carried out in a microwave reactor at 150 °C for 15–25 minutes. The reaction progress was monitored by TLC (Sorbfil, ethyl acetate/hexane, 2 : 1). The solvent was then removed under reduced pressure, and the product was purified by column chromatography on aluminum oxide using an ethyl acetate/petroleum ether mixture (1 : 10) as the eluent.

Dimethyl 9,10-dimethoxy-1-oxo-11b-phenyl-5,6,7,11b-tetrahydro-1*H*-pyrrolo[2,1-*a*][2]benzazepine-2,3-dicarboxylate (4a). Yield: 93 mg (83%), yellow oil. ^{1}H NMR (600 MHz, $CDCl_3$), δ = 1.80–1.92 (m, 2H, 6-CH_2), 2.60–2.64 (m, 1H, 7-CH_2), 2.84–2.88 (m, 1H, 7-CH_2), 3.57 (t, 2H, 5-CH_2, J = 6.6 Hz), 3.77 (s, 3H, OCH_3), 3.82 (s, 3H, OCH_3), 3.88 (s, 3H, CO_2CH_3), 4.05 (s, 3H, CO_2CH_3), 6.63 (s, 1H, H-11), 6.98 (dd, 2H, J = 2.5, 8.1 Hz, H-Ar), 7.31–7.34 (m, 3H, H-Ar), 7.43 (s, 1H, H-8). ^{13}C NMR (150 MHz, $CDCl_3$), δ = 26.7, 33.0, 47.5, 51.6, 53.9, 56.0, 56.2, 81.9, 100.0, 113.3, 114.3, 124.4, 127.8 (2C), 128.8, 129.2 (2C), 134.1, 137.2, 147.1, 148.5, 162.2, 163.5, 170.5, 194.6. MS (LCMS), m/z: 452 $[M + H]^+$. Found, $C_{25}H_{25}NO_7$, exact mass: 451 (%): C, 66.65; H, 5.67; N, 3.15. Anal. calcd (%): C, 66.51; H, 5.58; N, 3.10.

Spectral data for the remaining compounds are given in the SI.

Cell culture and cell viability assay

The obtained compounds underwent primary bioscreening to assess cytotoxic activity. The testing was conducted at the Federal State Budgetary Institution "Institute of Physiologically Active Compounds of the Russian Academy of Sciences (IPAC RAS)" by Senior Researcher L. V. Anikina. The primary evaluation of the compounds' cytotoxic activity was performed on the following human cell cultures: A549 (lung carcinoma, ATCC CCL-185), HCT116 (colorectal carcinoma, ATCC CCL-247), RD (rhabdomyosarcoma, ATCC CCL-136), and HeLa (cervical adenocarcinoma, ATCC CCL-2). These cell lines were obtained from the Institute of Cytology RAS, Saint Petersburg (Russian Collection of Cell Cultures of Vertebrates), and HCT116 was additionally obtained from the Bioresource Collection of Cell Lines and Primary Tumors of the N.N. Blokhin National Medical Research Center of Oncology, Moscow. The test results are presented below (Table 3). Cytotoxicity of the synthesized compounds **3a–i** and **4a** against RD (rhabdomyosarcoma), HCT116 (intestinal carcinoma), HeLa (cervical adenocarcinoma), A549 (lung carcinoma) was determined by the 3-(4,5-

dimethylthiazol-2-yl)-2,5-diphenyltetrazolium bromide (MTT) assay. Cells were seeded at a concentration of 1×10^4 cells per 200 μl in a 96-well plate and cultured at 37 °C in a humidified atmosphere with 5% CO_2. After 24 hours of incubation, various concentrations of the tested compounds (from 100 to 1.56 μM l^{-1}) were added to the cell cultures and then the cells were cultured under the same conditions for 72 hours. Each concentration was performed in triplicate. All substances were dissolved in DMSO, the final concentration of DMSO in the well did not exceed 0.1% and was not toxic to cells. The control wells were wells to which the solvent was added at a final concentration of 0.1%. After incubation, 20 μl of MTT (5 mg ml^{-1}) were added to each well and the plates were incubated for another 2 hours. Then the medium was removed from the plates and 100 μl of DMSO was added to each well to dissolve the formed formazan crystals. Optical density at 536 nm was determined using a Cytation3 plate analyzer (BioTek Instruments, Inc.). The concentration value causing 50% inhibition of cell population growth (IC_{50}) was determined from dose–response curves using OriginPro 9.0 software.

Nitric oxide assay

RAW 264.7 macrophage cells (ATCC®-TIB-71™) were cultured in Dulbecco's Modified Eagle Medium (DMEM) added by 10% fetal bovine serum (FBS), 100 U penicillin per ml, 100 μg streptomycin per ml, and 0.25 μg gibco amphotericin B per ml. The cells were plated in 96-well plates at 2×10^5 cells per well and incubated for 24 hours at 37 °C under 5% carbon dioxide (CO_2). Then the culture medium was replaced by DMEM without FBS, and the cells were incubated for 3 hours. The cells were continued to pre-treat with compounds **3a–b**, **3d–g**, **3i**, **2a–b**, **1a** and L-NG-methyl arginine acetate (L-NMMA) as a positive control at 256, 64, 16, and 4 μg ml^{-1} for 2 h, followed by treatment with 10 μg ml^{-1} lipopolysaccharides (LPS) for 24 hours. The levels of NO production were assessed by the Griess Reagent System (Promega Corporation, WI, USA), and L-NMMA (Sigma) was used as a reference. The nitrile concentration in the medium was determined by measuring the absorbance at 540 nm (A_{540}) in a microplate reader. The standard curve was generated based on the concentrations of $NaNO_2$. Each experiment was examined in triplicate. Half-maximal inhibitory concentration (IC_{50}) for the inhibition of NO production were calculated by TableCurve 2Dv4. To determine the viability of RAW 264.7 cells, MTT (3-(4,5-dimethylthiazol-2-yl)-2,5-diphenyltetrazolium bromide) assay was performed.

Molecular docking study

To investigate the relationship between structure and cytotoxicity, the molecular docking was performed. The crystal structures of topoisomerase IIb (PDB ID: 3QX3) in complex with DNA and etoposide (PDB ID: EPV) were retrieved from the protein data bank (https://www.rcsb.org/structure/3QX3). This structure was solved by X-ray crystallography at 2.16 Å resolution. For the preparation of protein, water molecules, ligands, and heteroatoms were removed. Polar hydrogens and Kollman charges were then added. Structures of ligands were built by Chem3D and converted into *.pdbqt format after structural optimization. The grid box was set with grid spacing 0.375 Å and a grid volume of 40 × 40 × 40 Å. The docking protocol was validated by redocking etoposide into the binding pocket of the receptor which showed RMSD of 0.522 Å and docking score of −13.6 kcal mol^{-1}. The main interactions were revealed as the co-crystallized ligand, including hydrogen bonds with Asp479, Gly478, DC8, DG10, and DG13; pi–pi stacked and pi–alkyl bonds with Arg503, DG13. Next steps, the synthesized compounds were docked into the same binding site of etoposide with the receptor. The top nine poses were generated in which a more negative binding energy and zero RMSD were selected as the best pose. The ligand–receptor interactions were visualized using Discovery Studio 2021. The molecular docking was performed using AutoDockTools 1.5.7 software. The calculation has been conducted using an Intel® Core™ i3-10400 CPU @ 2.90 GHz workstation.

Conclusions

In summary, the effective synthesis of pyrrolo[2,1-*a*][2]benzazepine and indolo[2,1-*a*][2]benzazepine derivatives through on domino reaction of 1-aroyl-4,5-dihydro-3*H*-[2]benzazepines and electron-deficient alkenes and alkynes has been described. All synthesized compounds **3a–g**, **4a** and **3h,i** were evaluated for *in vitro* anticancer activity against four representatives, rhabdomyosarcoma (RD), intestinal carcinoma (HCT116), cervical adenocarcinoma (HeLa), lung carcinoma (A549) cell lines as well as anti-inflammatory activity. Compounds **3b–e** had remarkable inhibitory activity against the tested cancer cell lines with IC_{50} values of 4.52 to 19.97 μM. For anti-inflammatory activity, compound **3b** showed the most potent inhibitory effect on NO production, with an IC_{50} value of 19.1 ± 1.2 μM. Molecular docking simulations revealed significant interactions of **3b–3e** compounds with residues in the etoposide-binding site of topoisomerase. These preliminary results suggest that 6,7-dihydro-5*H*-pyrrolo[2,1-*a*][2]benzazepine compounds are worthy of further study aiming to develop new potential anticancer agents.

Author contributions

Conceptualisation, A. A. N., T. A. D. T., T. N. B., A. V. V. and L. G. V.; methodology, A. A. N., E. Yu. N., A. A. T., L. V. A., and T. A. D. T. All authors have read and agreed to this version of the manuscript.

Conflicts of interest

There are no conflicts to declare.

Data availability

The datasets supporting this article have been uploaded as part of the supplementary information (SI). Supplementary information is available. See DOI: https://doi.org/10.1039/d5ra09014h.

Acknowledgements

This work has been funded by the Russian Science Foundation (Project No. 24-43-04003) and Vietnam Academy of Science and Technology (Project No. QTRU06.02/24-26).

Notes and references

1 N. M. Fahmy, E. Al-Sayed, M. El-Shazly and A. Nasser Singab, *Nat. Prod. Res.*, 2020, **34**, 1891–1912.
2 D. F. Rambo, R. Biegelmeyer, N. S. B. Toson, R. R. Dresch, P. R. H. Moreno and A. T. Henriques, *Phytother Res.*, 2019, **33**, 1258–1276.
3 W. K. Anderson, A. R. Heider, N. Raju and J. A. Yucht, *J. Med. Chem.*, 1988, **31**, 2097–2102.
4 J. Habermann, E. Capitò, M. d. R. R. Ferreira, U. Koch and F. Narjes, *Bioorg. Med. Chem. Lett.*, 2009, **19**, 633–638.
5 B. Zhang, Z. Nikolovska-Coleska, Y. Zhang, L. Bai, S. Qiu, C. Y. Yang, H. Sun, S. Wang and Y. Wu, *J. Med. Chem.*, 2008, **51**, 7352–7355.
6 S. M. C. Pelletier, P. C. Ray and D. J. Dixon, *Org. Lett.*, 2009, **11**, 4512–4515.
7 K. A Jebali, A. Planchat, H. Amri, M. Mathé-Allainmat and J. Lebreton, *Synthesis*, 2016, **48**, 1502–1517.
8 A. Y. Obydennik, A. A. Titov, A. V. Listratova and A. V. Varlamov, *Tetrahedron*, 2025, **176**, 134524.
9 A. A. Nevskaya, A. R. Miftyakhova, L. V. Anikina, T. N. Borisova, A. V. Varlamov and L. G. Voskressensky, *Tetrahedron Lett.*, 2021, **87**, 153552.
10 M. D. Matveeva, T. N. Borisova, A. A. Titov, L. V. Anikina, S. V. Dyachenko, G. S. Astakhov, A. V. Varlamov and L. G. Voskressensky, *Synthesis*, 2017, **49**, 5251–5257.
11 M. D. Matveeva, A. Golovanov, T. Borisova, A. Titov, A. Varlamov, A. Shaabani, A. Obydennik and L. Voskressensky, *Mol. Catal.*, 2018, **461**, 67–72.
12 A. A. Ershova, A. D. Zinoveva, T. N. Borisova, A. A. Titov, A. V Varlamov, L. G. Voskressensky, V. T. Nguyen and T. Anh, *Tetrahedron Lett.*, 2019, **60**, 5.
13 A. D. Zinoveva, T. N. Borisova, P. A. Politova, A. A. Titov, A. V. Varlamov, L. G. Voskressensky, V. T. Nguyen and T. A. Le, *ChemistrySelect*, 2020, **5**, 10821–10826.
14 A. D. Zinoveva, T. N. Borisova, A. A. Titov, V. V. Ilyushenkova, V. B. Rybakov, E. A. Sorokina, A. V. Varlamov and L. G. Voskressensky, *Synth. Commun.*, 2022, **52**, 2311–2321.
15 A. D. Zinoveva, V. A. Podchufarova, T. N. Borisova, A. P. Novikov, O. V. Levitskaya, A. A. Titov, Y. I. Gaponenko, T. A. Dang Thi, D. Thi Nhung, L. T. Anh, T. Van Nguyen, A. V. Varlamov and L. G. Voskressensky, *Asian J. Org. Chem.*, 2025, **14**, 3–10.
16 Z. Vincze, A. B. Bíró, M. Csékei, G. Timári and A. Kotschy, *Synthesis*, 2006, 1375–1385.
17 L. G. Voskressensky, T. N. Borisova, M. D. Matveeva, V. N. Khrustalev, A. A. Titov, A. V. Aksenov, S. V Dyachenko and A. V. Varlamov, *Tetrahedron Lett.*, 2017, **58**, 877–879.